Interplay between Microscopic Diffusion and Local Structure of Liquid Water

Alessandro Cunsolo,*,† Andrea Orecchini,‡,§ Caterina Petrillo,§ and Francesco Sacchetti§

Brookhaven National Laboratory-National Synchrotron Light Source-II, P.O. Box 5000 Upton, New York 11973, United States, Institut Laue-Langevin, F-38042 Grenoble CEDEX 9, France, Dipartimento di Fisica, Università di Perugia, I-06123 Perugia, Italy, and CNR-INFM, Centro di Ricerca e Sviluppo SOFT, I-00185 Roma, Italy

Received: August 5, 2010; Revised Manuscript Received: October 30, 2010

We present a quasielastic neutron scattering (QENS) study of single-particle dynamics in pure water, measured at temperatures between 256 and 293 K along an isobaric path at 200 MPa. A thorough analysis of the spectral line shapes reveals a departure from simple models of continuous or jump diffusion, with such an effect becoming stronger at lower temperatures. We show that such a diverging trend of dynamical quantities upon cooling closely resembles the divergent (anomalous) compressibility observed in water by small-angle diffraction. Such an analogy suggests an interesting interplay between single-particle diffusion and structural arrangements in liquid water, both bearing witness of the well-known water anomalies. In particular, a fit of dynamical parameters by a Vogel−Tammann−Fulcher law provides a critical temperature of about 220 K, interestingly close to the hypothesized position of the second critical point of water and to the so-called Widom line.

Introduction

A full understanding of both structural and dynamical processes occurring in water at microscopic scales and driving to the well-known, still mysterious thermodynamic and transport anomalies represents an open challenge for condensed matter physicists.[1] Despite remarkable improvements achieved in both computational and experimental methods, as well as a thorough theoretical effort, which provided considerable progress in understanding the behavior of water,[2] even new complex features arose. Only to mention a noticeable example, the temperature dependence of properties such as compressibility, specific heat, and volume expansivity[3] seems featured by an unexplained apparent divergence as long as the homogeneous nucleation temperature is approached from above.[4]

Originally, from the theoretical side, various models have been invoked to account for the above-mentioned anomalous enhancement of thermodynamic properties, and they can be essentially split into three broad categories: (i) models based on the so-called "stability limit conjecture", which ascribe the divergent trend to the proximity of a spinodal line re-entering from the negative pressure portion of the phase diagram;[5] (ii) models assuming the existence of a second critical point at the end of a liquid−liquid coexistence line, the so-called Widom line, separating two polymorphic phases of water;[6] and (iii) singularity-free models, simply ruling out the occurrence of any singularity and rather predicting a systematic growth toward finite values.[7] Recently some progress has been made in analyzing the different scenarios even if no definite conclusion has been drawn,[4,8−11] apart from the evidence that a strongly anomalous behavior is present in many observed quantities toward 220 K and 200 MPa.[4] Additional indications for the presence of a complex structural evolution in the water phase diagram have been also gained from a recent small-angle X-ray scattering experiment.[12,13]

In a previous work we employed quasielastic neutron scattering (QENS) to measure the single-particle response of water as a function of pressure[14] and thus highlighted the need for a more accurate modeling of the intermediate scattering function (ISF) in the picosecond time scale. Indeed, it was found that an ISF based on the stretched exponential model,[8,9,15] instead of simple exponential functions, could fit the experimental data to a significantly better extent in the explored temperature (268 K) and pressure (from 80 to 350 MPa) region. The stretched exponential function is indeed particularly useful to highlight small deviations from the more traditional single-exponential model,[16] since it contains the latter as a specific case. The more accurate fit provided by the stretched exponential model suggested the existence of a dynamic counterpart[17] of the diffraction data[12] supporting the liquid−liquid transition hypothesis. Indeed, the detailed line-shape analysis with a stretched-exponential model revealed an unexpected behavior of the translational relaxation time $\tau_{av}(Q)$ at low momentum transfer Q. Surprisingly we found a relation between such an anomalous trend of $\tau_{av}(Q)$ and the structural anomaly already observed in water by both neutron[18] and X-ray[12,19] diffraction, essentially consisting in a low-Q growth of the coherent static structure factor $S(Q)$.

This result is far from being easily interpreted, since none of the existing models predicted it, and available simulation results are not accurate enough to confirm its presence.[8,9,12,15] However, this effect has rather fundamental physical implications, since: (i) it establishes a direct link between a single-particle incoherent property and a collective coherent one like $S(Q)$; (ii) it demonstrates a remarkable interplay between self-dynamics and structure.

To get more information about the observed effect on the diffusion process,[17] we extended the previous experiment by measuring the QENS spectra of water at new thermodynamic points inside the liquid equilibrium region, namely, at the constant pressure of 200 MPa and temperatures between 256

* To whom correspondence should be addressed. E-mail: acunsolo.bnl.gov.
† Brookhaven National Laboratory-NSLS-II.
‡ Institut Laue Langevin.
§ Università di Perugia and CNR-INFM.

10.1021/jp1073768
Published on Web 11/29/2010

and 293 K. This isobaric path deserves particular interest because it lays roughly at the boundary of the transition between ice I and ice III. In addition, the set of measured temperatures points from above toward the region where the density minimum was recently observed in confined water at normal pressure.[20]

Experimental Method and Data Analysis

As in our previous work, the new experiment was performed using the time-of-flight, cold neutron spectrometer IN5 operating at the high-flux reactor of the Institut Laue Langevin in Grenoble. The same experimental conditions were chosen, that is, an incident wavelength of 8.5 Å and an energy resolution of 24 μeV. The same raw-data reduction of the previous paper was applied,[14] which, besides standard subtraction of environmental background and sample holder scattering, included a thorough evaluation of multiple scattering arising by both sample and sample holder.

The resulting experimental intensity $I^{\mathrm{exp}}(Q, \omega)$, proportional to the incoherent dynamic structure factor $S_{\mathrm{inc}}(Q, \omega)$, can be modeled as follows:

$$I^{\mathrm{exp}}(Q,\omega) = \frac{k}{k_0}\frac{1}{2\pi\hbar}A(Q) \times \int_{-\infty}^{+\infty} e^{i\omega t} F_{\mathrm{mod}}(Q,t)\, \mathscr{R}(t)\, \mathrm{d}t + b(Q) \quad (1)$$

where $\hbar\omega$ is the exchanged energy, k_0 and k are the incoming and outgoing neutron wave vector, respectively, $F_{\mathrm{mod}}(Q, t)$ is the ISF model we will use, and $\mathscr{R}(t)$ is the Fourier transform of the instrumental resolution function, which can be accurately modeled by a Gaussian line. The constant $A(Q)$ is a Debye−Waller-like scale factor, and $b(Q)$ accounts for possible residual background. The model adopted in the following to describe the ISF $F_{\mathrm{mod}}(Q, t)$ relies upon the assumption of a mutual decoupling between translational and rotational degrees of freedom. Indeed such an approximation has been successfully applied to previous QENS data on supercooled,[21] supercritical,[22] and confined[23] water. Moreover, molecular dynamics (MD) simulations in the supercooled phase[15,24] demonstrated that the rotational contribution to the ISF is rather small, at least in the low-Q region accessed in the present experiment.

Based upon the above arguments, we assumed the ISF to be the product of two uncoupled terms:

$$F_{\mathrm{mod}}(Q,t) = \exp\left\{-\left[\frac{t}{\tau_T(Q)}\right]^{\beta_T(Q)}\right\} \times \sum_{l=0}^{l_{\max}} (2l+1) j_l^2(Qd) \exp\left\{-\frac{l(l+1)}{2}\left[\frac{t}{\tau_R(Q)}\right]^{\beta_R(Q)}\right\} \quad (2)$$

The first term represents translational motions by a stretched exponential function of relaxation time $\tau_T(Q)$ and stretching exponent $\beta_T(Q)$, according to the prescriptions of the so-called relaxing cage model.[15,25,26] Rotational motions are instead described by the summation over l, which involves products of a stretched exponential with the l-th order spherical Bessel function, where the rotation radius d is here approximated by the O−H bond length (0.98 Å).

Following the prescription of ref 24, this second term mainly consists in a generalization of the Sears' model for the spectral response of a free rotator.[16] The simple exponentials appearing in the Sears' expansion are here replaced by stretched exponential functions, with stretching parameter $\beta_R(Q)$ and relaxation time $\tau_R(Q)$. This model has a clearly hybrid character, as it merges two somehow conflicting approaches: the relaxing cage model, which implicitly assumes a coupling between degrees of freedom, and the Sears' model, rigorously holding only for free rotators. However, this description has proven to provide a consistent, yet merely phenomenological, account of the diffusive dynamics of water.[24] In addition, it is worth recalling that the stretched-exponential model contains the simple-exponential model[16] as a particular case, that is, when the stretching exponent β equals 1. Therefore, a robust fitting procedure would either recover the value $\beta = 1$ in case the standard diffusion model[16] can reproduce the data sufficiently well, or highlight more complex data trends. Finally a stretched exponential function mimics the possible presence of many simple relaxation processes described by many Lorentzian functions, thus being a generalization of the Sears' approach with a minimum additional number (just one) of parameters.

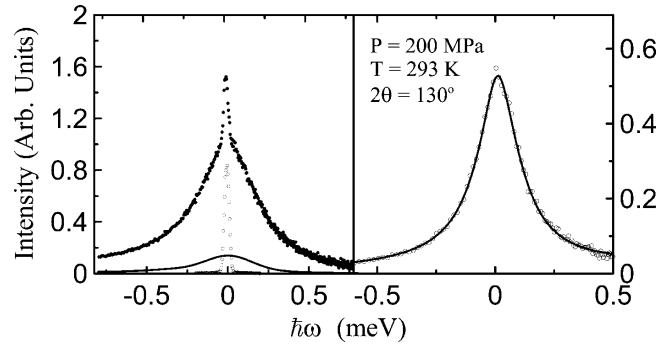

Figure 1. Left panel, typical experimental data (full circles) as compared to the multiple scattering contribution (full line) and the instrument resolution (empty circles). Right panel, corrected intensity (empty circles) and model fit (full line) described in the text.

The quasielastic portion of the measured spectra was fitted with the model of eqs 1 and 2 by leaving free to vary the parameters $A(Q)$, $b(Q)$, $\tau_T(Q)$, $\beta_T(Q)$, $\tau_R(Q)$, and $\beta_R(Q)$. In particular the fit was restricted to the symmetric energy region -0.6 meV $\ll \hbar\omega \ll 0.6$ meV, to avoid contaminations of the quasielastic line shape by the onset of a nonconstant contribution by the density of states (DOS) of water. Indeed the first DOS peak in water is centered at about 6 meV, with a low-energy tail extending down to ~1 meV. The first few trials clearly revealed that the rotational terms having $l > 3$ could be safely neglected, in agreement with ref 24.

The good agreement between experimental data and fitted model function is evident from the right panel of Figure 1, which is just an example of the typical result obtained at all Q values and temperatures. However, to get a more quantitative assessment of the validity of the model function in eq 2, we performed a second fit to the data, with exactly the same set of numerical routines, by fixing $\beta_T(Q) = 1$ and $\beta_R(Q) = 1$, which restores the more conventional approach based on simple exponentials.[16] The second fit was systematically slightly worse than the first one employing the full model of eq 2, as actually already observed in ref 14.

Nonetheless, for a more grounded choice of the best-suited model function, we performed a further analysis, based on a Bayesian approach to derive a ratio between the posterior probabilities for the two models, namely, the full model of eq 2 and the conventional one with $\beta_T(Q) = 1$ and $\beta_R(Q) = 1$, given the experimental data. Such an approach, outlined by Sivia,[27] has already been successfully applied to similar neutron scattering experiments.[28,29] In general, the posterior probability $P(H|D, I)$ of the hypothesized model H, conditioned by the data

D and the possible previous information I, is $P(H|D, I) \propto P(D|H, I)P(H|I)$, where $P(H|I)$ is the prior probability of hypothesis H and $P(D|H, I)$ is the probability of the data D, given the hypothesis H. The latter can be reasonably taken as the likelihood function of the data, obtained by performing the fit with the model derived from H.[27−29] Such a likelihood function can be approximated by $L(D|H) \propto \exp(-\chi^2/2)$, where χ^2 is the chi-square corresponding to the fit obtained under the hypothesis H. If we now assume hypothesis H_1 to be the model of eq 2 and hypothesis H_2 to be the conventional model, we can safely assume $P(H_1|I)/P(H_2|I) \geq 1$, because H_1 is more general than H_2. As a consequence, the ratio between the posterior probabilities of the two models is $P(H_1|D, I)/P(H_2|D, I) = \exp[(\chi_2^2 - \chi_1^2)/2]$ which, being $\chi_1^2 = 840$ and $\chi_2^2 = 940$ on average (over Q), definitely favors H_1 against H_2 by a factor of the order of exp(50). This result confirms also the suggestion of MD simulations.[15] Finally it is important to stress that the major difference between the two models is confined to the tail region and only a high-accuracy experiment can be sensible enough to distinguish the stretched exponential ISF from a normal exponential ISF. In addition the difference is confined to the low-temperature region since $\beta_T(Q)$ approaches unity on increasing the temperature.

On the basis of the above arguments, the model of eq 2 was preferred to describe the present data. The fit results show that the quasielastic line shape in the present energy range is largely dominated by the translational component, which is fully accounted for by the two fit parameters $\tau_T(Q)$ and $\beta_T(Q)$. A widely informative quantity one can derive from τ_T and β_T is the average *translational* relaxation time, defined as:[23]

$$\tau_{av}(Q) = \int_0^\infty dt \exp\left\{-\left[\frac{t}{\tau_T(Q)}\right]^{\beta_T(Q)}\right\} \qquad (3)$$

Best fit values of the translational relaxation rate $\Gamma_T(Q) = 1/\tau_{av}(Q)$ and of $\beta_T(Q)$ are reported in Figure 2 as a function of Q^2, for the various temperatures investigated. At the highest temperatures, $\beta_T(Q)$ equals 1 at almost all of the explored wavevector transfers, except in the low-Q region ($Q^2 \lesssim 0.4$ Å^{-2}) where a neat departure from unity is observed. Upon cooling, the crossover from the stretched to the simple-exponential regime moves toward higher Q-values. The relaxation rate $\Gamma_T(Q)$ roughly follows a Q^2 dependence, as expected for continuous or jump diffusion at such low Q-values. Nevertheless, an anomalous deviation from the quadratic trend is visible for $Q^2 \lesssim 0.4$ Å^{-2} and becomes more and more evident at lower temperatures. Such an anomaly is completely absent if the fit is performed using the conventional simple-exponential model, in agreement with what was found in the previous work at different thermodynamic states.[14] On a speculative ground, the systematic decrease with temperature of the stretching parameter, or equivalently the broadening of the distribution of relaxation times, might be connected to a mode coupling between diffusive dynamics and some internal degrees of freedom, as also highlighted by MD simulations.[8,9]

As to the rotational contribution, it is fairly small in the reduced Q-range of the experiment. On the other hand such a limited Q range is needed to measure the self-dynamic structure factor with the desired high energy resolution. Therefore, the fit provides only an approximate determination of $\tau_R(Q)$ and $\beta_R(Q)$. In particular the stretching exponent $\beta_R(Q)$ is found to be systematically equal to 1, thus retrieving the conventional behavior at all temperatures and wavevector transfers. The rotational time $\tau_R(Q)$ results to be of about 75 ps, slightly increasing to 80 ps upon cooling, although with an average error of the order of 20 ps. As a consequence, no additional quantitative information can be derived from the rotational part without exploring a wider Q region.

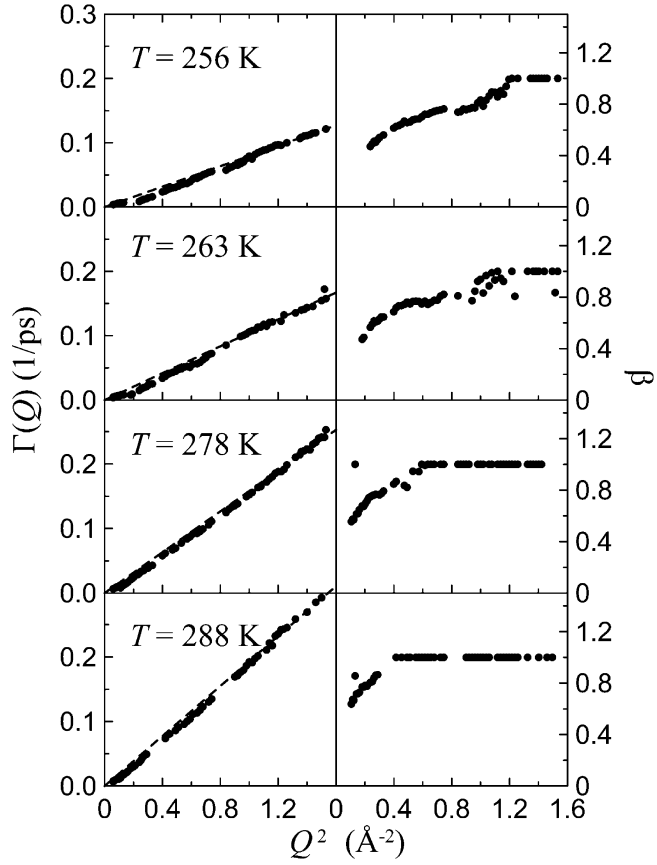

Figure 2. Momentum dependence of the relevant parameters $\Gamma_T(Q)$ (left) and $\beta_T(Q)$ (right) obtained by fitting the spectral line shapes as described in the text. The polynomial fit by eq 5 (see text) to the parameter $\Gamma_T(Q)$ is also shown as a dashed line.

Discussion

Under the assumption that the rotational contribution is negligible, we observe that $\tau_{av}(Q) = S_{inc}(Q, 0)$, a quantity usually referred to as the elastic incoherent structure factor (EISF). This implies that the dynamical quantity $\tau_{av}(Q)$ contains some information about the spatial distribution of the diffusion process at long time. In the case of simple diffusion $\tau_{av}^{SD}(Q) = 1/DQ^2$, D being the diffusion constant. As a measure of the departure from this simple trend of continuous diffusion, it is reasonable to introduce the structure function $S_{dyn}(Q)$ defined as:

$$S_{dyn}(Q) = \tau_{av}(Q)/\tau_{av}^{SD}(Q) = S_i(Q, 0)DQ^2 \qquad (4)$$

To determine $S_{dyn}(Q)$ we can either use the diffusion constant D as deduced by a direct NMR measurement[30] or determine it by an appropriate fit of the present $\Gamma_T(Q)$ data. In the low-Q region where the simple relationship $DQ^2 = \Gamma_T$ holds, the present data show the observed anomalous trend, and therefore no safe derivation of D is possible, also because the spectral line width becomes small and comparable to the experimental resolution. On the other hand the high-Q data displaying a more regular behavior might well be exploited to this aim, provided that at least a higher-order Q^4 term is considered for extending the simple diffusion law to larger Q's. With such arguments in mind

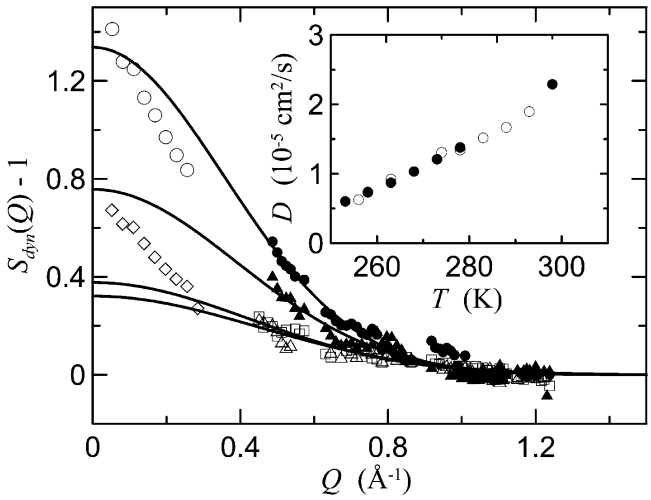

Figure 3. Momentum dependence of the structure function $S_{dyn}(Q) - 1$ at selected temperatures as follows: 256 K dots, 263 K full triangles, 278 K empty squares, and 288 K empty triangles. For comparison, empty circles and empty diamonds report the anomalous component of the structure factor of water measured by SAXS, respectively at 239 and 273 K along the coexistence line.[19] The full lines refer to the fit described in the text. In the inset the diffusion constant obtained from the fit of eq 5 (dots) and from the NMR experiment[30] (circles) are reported.

the present $\Gamma_T(Q)$ data were fitted for $Q \geq 0.78$ Å^{-1} by the phenomenological equation

$$\Gamma_T(Q) = DQ^2 + KQ^4 \tag{5}$$

where the term KQ^4 takes into account possible deviations from the Q^2-trend due to the relatively high-Q range considered. Such a correction term results to contribute to a small amount, never exceeding 20% at the highest Q and smallest temperature, which is nonetheless necessary to obtain values of D in good agreement with NMR results[30] (see the inset of Figure 3). The structure function $S_{dyn}(Q)$ was finally calculated by eq 5 using the D-values obtained by the above polynomial fit on $\Gamma_T(Q)$. A set of data for $S_{dyn}(Q)$ is reported in Figure 3 where it is seen that the structure function increases at low Q, with such an effect being more evident at low T.

To get a quantitative information on the temperature dependence, $S_{dyn}(Q)$ can be fitted to a Gaussian model function as follows:

$$S_{dyn}(Q) = [S_{dyn}(0) - 1]\, e^{-(1/6)\langle R^2\rangle Q^2} + 1 \tag{6}$$

where $S_{dyn}(0)$ is a scale factor and the mean square radius $\langle R^2\rangle$ provides a measure of the spatial extension of the dynamical anomaly observed in $S_{inc}(Q, 0)$. The fits with this model are of good quality at all temperatures, with $\langle R^2\rangle^{1/2}$ decreasing from 4.9 Å at 256 K to 4.2 Å at 293 K. The corresponding best-fit curves are shown in Figure 3 and compared with the anomalous component $S_a(Q)$ of the static structure factor, as determined by small angle X-ray scattering (SAXS) measurements at 239 and 273 K along the coexistence line.[19] The latter is here normalized to the zero-wavevector limit of the normal (nondiverging) component of the static structure factor,[19] that is $S_n(Q = 0) = \rho k_B T \kappa_T^n$, where ρ is the number density, k_B is the Boltzmann constant, and κ_T^n is the normal isothermal compressibility.[31] Although no adjustable scaling factor has been used, a fair agreement is readily observed, thus extending the result already obtained in our previous work[17] to the new thermodynamic region explored herewith. Therefore, some relationship is established between a collective coherent property, that is, $S_a(Q)$ as measured by X-ray diffraction experiments, and a merely incoherent one, that is, $S_{dyn}(Q)$ measured in the present QENS experiment and connected to the elastic incoherent structure factor $S_{inc}(Q, 0)$. This apparently surprising result is however consistent with the foundations of the so-called relaxing cage model, which involves a coupling between single-particle diffusion and local arrangement of the first neighbors cage. Finally it is important to observe that $S_{dyn}(0) - 1$ continuously increases as the temperature is lowered, in a way similar to what observed in diffraction experiments at normal pressure.[12,19,32] Also, as found in the same diffraction experiments, $\langle R^2\rangle^{1/2}$ shows a weak temperature dependence, indicating that the size of the regions involved in the observed increase of $S_{dyn}(Q)$, and possibly of $S_a(Q)$, is probably related to the molecular size.

The increasing trend of both $S_{dyn}(0)$ and $S_a(Q)$ upon lowering the temperature is quite intriguing and deserves further analysis. In particular it might be put in relationship with the hypothesized liquid−liquid critical point,[6] or similar transition point,[4] usually located at 220 K and 200 MPa. To this end, the temperature dependence of $S_{dyn}(0)$ can be fitted by empirical models currently adopted in literature for describing similar diverging trends, such as the critical law, well-adapted to the trend of susceptibility close to a critical point:

$$S_{dyn}(0, T) = \frac{K}{(T - T_c)^\gamma} \tag{7}$$

or the Vogel−Tammann−Fulcher (VTF) law,[33−35] usually employed to describe the trend of the relaxation time close to the glass transition in vitreous substances:

$$S_{dyn}(0, T) = K \exp\left[\frac{\Delta E}{k_B(T - T_c)}\right] \tag{8}$$

In both models, K is a scaling factor, T_c the critical temperature, γ the so-called critical exponent, and ΔE the VTF characteristic energy providing a measure of the structural "strength" of the system.[36] A fitting procedure where all of these parameters were left free to vary produced the results reported in Figure 4, which shows that both models provide a good description of the experimental data. It is worth to note that both the critical and the VTF equations are here exploited in a purely phenomenological way. In particular, the VTF equation is customarily used to describe the temperature evolution of viscosity in glass formers and might thus appear quite unsuited for a liquid like water. Nevertheless, the VTF law is known to correctly describe the temperature dependence of orientational correlation times or of the diffusion constant in supercooled water over a wide range of temperatures and pressures.[26]

According to the above fits, it is found that the critical model produces a quite unphysical exponent $\gamma = 1.26 \pm 0.10$. In addition the critical temperature turns out to be $T_c = 241 \pm 5$ K, which is quite far from the measured temperatures, considering that the critical model has a general validity only when T approaches T_c ($|T - T_c|/T_c \ll 1$). On the contrary, the empirical VTF model is valid to describe the temperature evolution of thermodynamical and dynamical quantities in principle at any temperature. The VTF fitting procedure yields a critical temperature $T_c = 218 \pm 5$ K, which is interestingly close to the

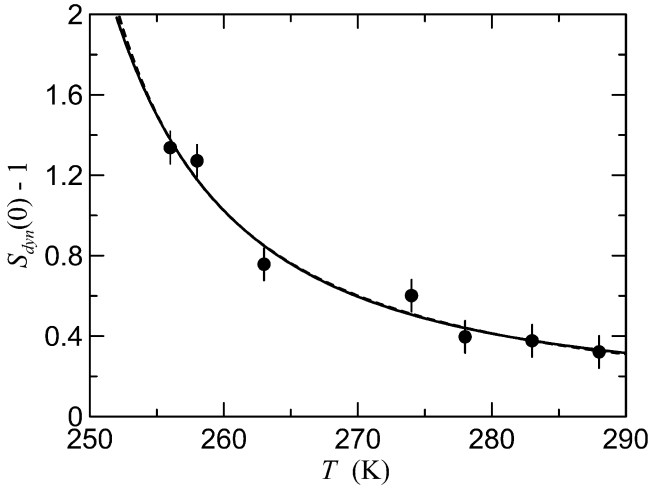

Figure 4. $S_{dyn}(0) - 1$ as a function of temperature (dots), compared to the fits described in the text: dashed line for the critical law, full line for the VTF law.

temperature where an intriguing density minimum has been recently observed by small angle neutron scattering[20] and hypothesized to be a signature of the Widom line.[6]

Conclusion

In conclusion, we presented here a QENS study of the temperature evolution of the single-particle dynamics of water along the 200 MPa isobar, which points toward the minimum temperature where liquid water exists. By paying special care to the data analysis, at low temperatures we observe a progressive and clear departure of the ISF from the simple-exponential relaxational behavior predicted in the continuum limit. Moreover, at a low exchanged momentum, namely, $Q \simeq 0.3-0.6$ Å^{-1}, we find that the relaxation time does not follow the expected Q^2 proportionality which usually fingerprints single-molecule free jump diffusion. These results reveal a complex interplay between single-particle diffusion and local structural rearrangements. In fact, the anomalous Q-dependence of the relaxation time parallels a similar trend of the static structure factor, where an unusual increase toward low-Q has been determined by small-angle X-ray diffraction.[12,19,32] Such finding appears rather interesting for two reasons. From one side the herewith presented QENS experiment intrinsically probes *single molecule* dynamics only, the influence of local structure being in principle observable only indirectly. Second, such an effect is more likely to be observed in highly viscous systems such as polymers or glass formers, where single-molecule jumps turn out to be strongly intertwined with the mesoscopic arrangement. Once again this stresses the anomalous character of large-scale connectivity in water and, intriguingly enough, also supports the hypothesis of a second critical point.[4] In fact the critical temperature obtained by fitting the temperature evolution of our data to a VTF equation turns out to be surprisingly close to the hypothesized position of the critical point.[37] Far from being an experimental observation of such an elusive effect, this result could nevertheless provide a further indication of the existence of the so-called Widom line,[6,20] which is expected to merge into the critical point. Therefore, the present analysis might open up a way to further investigations for probing the deeply supercooled state, usually reached by trapping the sample inside a geometrical confinement.[20]

References and Notes

(1) Angell, C. A. Supercooled water. In *Water-a comprehensive treatise*; Franks, F., Ed.; Plenum Press: New York, 1982; Vol. 7, Chapter 1.
(2) Debenedetti, P. G. *Metastable Liquids*; Princeton University Press; Princeton, NJ, 1997.
(3) Speedy, R. J.; Angell, C. A. *J. Chem. Phys.* **1976**, *360*, 851.
(4) Angell, C. A. *Science* **2008**, *319*, 582.
(5) Speedy, R. J. *J. Phys. Chem.* **1982**, *86*, 982. D'Antonio, M. C.; Debenedetti, P. G. *J. Chem. Phys.* **1986**, *86*, 2229.
(6) Poole, P. H.; Essmann, U.; Sciortino, F.; Stanley, H. E.; Mishima, O. *Nature* **1992**, *360*, 324. Poole, P. H.; Essmann, U.; Sciortino, F.; Stanley, H. E. *Phys. Rev. E* **1993**, *48*, 3799.
(7) Stanley, H. E.; Teixeira, J. *J. Chem. Phys.* **1980**, *73*, 3404.
(8) Starr, F. W.; Harrington, S.; Sciortino, F.; Stanley, H. E. *Phys. Rev. Lett.* **1999**, *82*, 3629.
(9) Starr, F. W.; Sciortino, F.; Stanley, H. E. *Phys. Rev. E* **1999**, *60*, 6757.
(10) Errington, J. R.; Debenedetti, P. G. *Nature* **2001**, *409*, 318.
(11) Stanley, H. E.; Kumar, P.; Xu, L.; Yan, Z.; Mazza, M. G.; Buldyrev, S. V.; Chen, S.-H.; Mallamace, F. *Physica A* **2007**, *386*, 729.
(12) Huang, C.; Wikfeldt, K. T.; Tokushima, T.; Nordlund, D.; Harada, Y.; Bergmann, U.; Niebuhr, M.; Weiss, T. M.; Horikawa, Y.; Leetmaa, M.; Ljungberg, M. P.; Takahashi, O.; Lenz, A.; Ojamäe, L.; Lyubartsev, A. P.; Shin, S.; Pettersson, L. G. M.; Nilsson, A. *Proc. Natl. Acad. Sci. U.S.A.* **2009**, *106*, 15214.
(13) Mallamace, F. *Proc. Natl. Acad. Sci. U.S.A.* **2009**, *106*, 15097.
(14) Cunsolo, A.; Orecchini, A.; Petrillo, C.; Sacchetti, F. *J. Chem. Phys.* **2006**, *124*, 084503.
(15) Chen, S.-H.; Gallo, P.; Sciortino, F.; Tartaglia, P. *Phys. Rev. E* **1997**, *56*, 4231.
(16) Sears, V. F. *Can. J. Phys.* **1966**, *44*, 1279.
(17) Cunsolo, A.; Orecchini, A.; Petrillo, C.; Sacchetti, F. *J. Phys.: Condens. Matter* **2007**, *19*, 415118.
(18) Bosio, L.; Teixeira, J.; Stanley, H. E. *Phys. Rev. Lett.* **1981**, *46*, 597.
(19) Xie, Y.; Ludwig, K. F.; Morales, G.; Hare, D. E.; Sorensen, C. M. *Phys. Rev. Lett.* **1993**, *71*, 2050.
(20) Liu, D.; Zhang, Y.; Chen, C.-C.; Mou, C.-Y.; Poole, P. H.; Chen, S.-H. *Proc. Natl. Acad. Sci. U.S.A.* **2007**, *104*, 9570.
(21) Chen, S.-H.; Teixeira, J.; Nicklow, R. *Phys. Rev. A* **1982**, *26*, 3477. Teixeira, J.; Bellissent-Funel, M. C.; Chen, S. H.; Dianoux, A. J. *Phys. Rev. A* **1985**, *31*, 1913.
(22) Tassaing, T.; Bellissent-Funel, M. C. *J. Chem. Phys.* **2000**, *113*, 3332.
(23) Zanotti, J. M.; Bellissent-Funel, M. C.; Chen, S.-H. *Phys. Rev. E* **1999**, *59*, 3084. Dellerue, S.; Bellissent-Funel, M. C. *Chem. Phys.* **2000**, *258*, 315.
(24) Liu, L.; Faraone, A.; Chen, S. H. *Phys. Rev. E* **2002**, *65*, 041506.
(25) Sciortino, F.; Gallo, P.; Tartaglia, P.; Chen, S.-H. *Phys. Rev. E* **1996**, *54*, 6331.
(26) Debenedetti, P. G. *J. Phys.: Condens. Matter* **2003**, *15*, R1669.
(27) Sivia, D. S. *Data Analysis - A Bayesian Tutorial*; Oxford Science Publications, Clarendon Press: Oxford, 2005.
(28) Bermejo, F. J.; Howells, W. S.; Jimenez-Ruiz, M.; Gonzalez, M. A.; Price, D. L.; Saboungi, M. L.; Cabrillo, C. *Phys. Rev. B* **2004**, *69*, 174201.
(29) Sacchetti, F.; Orecchini, A.; Cunsolo, A.; Formisano, F.; Petrillo, C. *Phys. Rev. B* **2009**, *80*, 024306.
(30) Harris, K. R.; Newitt, P. J. *J. Chem. Eng. Data* **1977**, *42*, 346.
(31) D'Arrigo, G.; Paparelli, A. *J. Chem. Phys.* **1988**, *88*, 405.
(32) Cunsolo, A.; Formisano, F.; Ferrero, C.; Bencivenga, F.; Finet, S. *J. Chem. Phys.* **2009**, *131*, 194502.
(33) Vogel, H. *Phys. Z.* **1921**, *22*, 645.
(34) Fulcher, G. S. *J. Am. Ceram. Soc.* **1925**, *6*, 339.
(35) Tammann, G.; Hesse, G. Z. *Anorg. Allg. Chem.* **1926**, *156*, 245.
(36) Dagdug, L. *J. Phys.: Condens. Matter* **2000**, *12*, 9573.
(37) Xu, L.; Kumar, P.; Buldyrev, S. V.; Chen, S.-H.; Poole, P. H.; Sciortino, F.; Stanley, H. E. *Proc. Natl. Acad. Sci. U.S.A.* **2005**, *102*, 16558.

JP1073768